




<b>Publication Year</b>	2022
<b>Acceptance in OA</b>	2025-03-14T15:23:28Z
<b>Title</b>	Qualification of the thermal stabilization, polishing and coating procedures for the aluminum telescope mirrors of the ARIEL mission
<b>Authors</b>	CHIOETTO, PAOLO, ZUPPELLA, PAOLA, Da Deppo, Vania, Pace, Emanuele, MORGANTE, GIANLUCA, TERENCE, Luca, BRIENZA, Daniele, Missaglia, Nadia, Bianucci, Giovanni, Spinelli, Sebastiano, GUERRIERO, Elisa, Rossi, Massimiliano, Grèzes-Besset, Catherine, Bondet, Colin, Chauveau, Grégory, Porta, Caroline, MALAGUTI, Giuseppe, MICELA, Giuseppina
<b>Publisher's version (DOI)</b>	10.1007/s10686-022-09852-x
<b>Handle</b>	<a href="http://hdl.handle.net/20.500.12386/36815">http://hdl.handle.net/20.500.12386/36815</a>
<b>Journal</b>	EXPERIMENTAL ASTRONOMY
<b>Volume</b>	53



# Qualification of the thermal stabilization, polishing and coating procedures for the aluminum telescope mirrors of the ARIEL mission

Paolo Chioetto<sup>1,2,3</sup>  · Paola Zuppella<sup>1,3</sup> · Vania Da Deppo<sup>1,3</sup> · Emanuele Pace<sup>4</sup> · Gianluca Morgante<sup>5</sup> · Luca Terenzi<sup>5</sup>, et al. [*full author details at the end of the article*]

Received: 30 September 2020 / Accepted: 23 March 2022 / Published online: 19 April 2022  
© The Author(s) 2022, corrected publication 2022

## Abstract

ARIEL, the Atmospheric Remote-sensing Infrared Exoplanet Large-survey, was selected as the fourth medium-class mission in ESA's Cosmic Vision program. ARIEL is based on a 1 m class telescope optimized for spectroscopy in the waveband between 1.95 and 7.8 micron and operating in cryogenic conditions. Fabrication of the 1.1 m aluminum primary mirror for the ARIEL telescope requires technological advances in the three areas of substrate thermal stabilization, optical surface polishing and coating. This article describes the qualification of the three procedures that have been set up and tested to demonstrate the readiness level of the technological processes employed. Substrate thermal stabilization is required to avoid deformations of the optical surface during cool down of the telescope to the operating temperature below 50 K. Purpose of the process is to release internal stress in the substrate that can cause such shape deformations. Polishing of large aluminum surfaces to optical quality is notoriously difficult due to softness of the material, and required setup and test of a specific polishing recipe capable of reducing residual surface shape errors while maintaining surface roughness below 10 nm RMS. Finally, optical coating with protected silver must be qualified for environmental stability, particularly at cryogenic temperatures, and uniformity. All processes described in this article have been applied to aluminum samples of up to 150 mm of diameter, leading the way to the planned final test on a full size demonstrator of the ARIEL primary mirror.

**Keywords** Aluminum mirrors · Opto-mechanical stabilization · Protected silver coating · Polishing · Cryogenic temperatures

---

Paolo Chioetto and Paola Zuppella contributed equally to this work.

---

## 1 Introduction

The main design drivers of the telescope for the ARIEL mission are a collecting area of at least  $0.6 \text{ m}^2$ , diffraction limited performance at a wavelength  $3 \mu\text{m}$  on a Field of View of  $30''$ , and an average throughput of 96% in the operating waveband of  $0.5 \mu\text{m}$  to  $8 \mu\text{m}$  [5, 11]. The telescope will operate at a temperature below 50 K.

To guarantee the desired throughput while keeping the size of the primary mirror small, an unobscured Cassegrain design was chosen, leading to an off-axis parabolic primary mirror featuring an elliptical aperture with major and minor axes measuring 1100 mm and 768 mm respectively.

In terms of optical performance, the diffraction limit requirement imposes the total wavefront error at the telescope exit pupil to be below 200 nm RMS, of which 160 nm RMS have been assigned as the primary mirror tolerance budget.

Aluminum alloy 6061, in the T651 temper, was chosen as construction material for the mirrors substrates and most of the supporting structures of the telescope, based primarily on JWST MIRI heritage Kroes et al. [18] and on consideration of manufacturability and cost [6].

Aluminum mirrors of such large size, operating at cryogenic temperatures in space, are however relatively untested, and present specific manufacturing challenges, related in particular to opto-mechanical stability of the substrate at cryogenic temperatures and polishing of the optical surface.

Aluminum is also prone to oxidation and its spectral reflectivity in the visible band does not lead to the required throughput, so a suitable protected coating with space heritage has been identified.

In order to demonstrate the viability of the manufacturing procedures selected for the primary mirror of ARIEL, a specific qualification campaign on substrate thermal stabilization, optical surface polishing and coating was conducted on samples of Al 6061-T651. Results of the campaign will then be translated to a full size prototype of the primary mirror (PTM) that will demonstrate the readiness level of the technologies employed.

This paper reports the results of the qualification campaign, starting from a description of the samples used in the qualification, and then presenting the three procedures under test.

### 1.1 Samples description

Aluminum samples of three different sizes have been used in the qualification activities: disks of 150 mm of diameter and 19 mm of thickness have been employed for machining, polishing and thermal stabilization tests; disks of 50 mm of diameter and 10 mm of thickness have been used for setup of the polishing process and finally disks of 25 mm of diameter, 6 mm of thickness, have been used for the coating qualification. All sample types have been cut from the same plate of rolled Al6061-T651 used for the PTM.

Additional glass samples (NBK-7), 25 mm of diameter by 4 mm of thickness, have been used for profilometry of the coating depth.

The 150 mm disks, four in total, have been used to qualify the thermal stabilization and polishing procedures. They have been machined flat before initiating the thermal cycles of the thermal stabilization procedure described in 2.2, and later underwent a series of polishing runs on a Lamplan M8400 flat lapping machine.

The first disk to be processed, identified as “LTU-1”, had been manufactured during Phase A of the ARIEL mission in 2017. It was then used to set up the thermal stabilization procedure and test it for the first time. The three remaining disks have been used to confirm the results and qualify the procedure since the outcome on LTU-1 was deemed satisfactory.

All aluminum samples and the PTM have been procured by MediaLario.<sup>1</sup>

## 2 Thermal stabilization

Dimensional stability is one of the main issues of aluminum as substrate material for cryogenic mirrors, especially when a large aperture is required, as is the case of ARIEL.

The purpose of a thermal stabilization procedure is to minimize residual substrate stresses that may be released during flight and final cool down of the telescope, causing an unpredictable variation of the shape of the optical surface of the mirrors that can ultimately affect optical performance.

The following paragraphs describe the sources of dimensional instability, identifying residual stress as the most prominent and actionable one, the stress release process that has been identified, adapted and tested, and the steps taken to verify compliance of the procedure with the program goals.

### 2.1 Sources of dimensional instability

There are four major types of dimensional instabilities that can affect optical performance of mirrors: temporal instability, thermal/mechanical hysteresis, thermal instability and other instabilities [1].

The first two are irreversible dimensional changes caused by the simple passage of time, or from changing mechanical or thermal environmental conditions. They are both caused by relaxation of residual stresses present in the material, and we expect them to be the main source of instability in aluminum mirrors.

The thermal stabilization procedure described here was identified and set up to tackle these two sources of instability.

“Thermal instability” refers to changes that are independent of the environmental change path, such as an intrinsic inhomogeneity in the coefficient of thermal

<sup>1</sup> Media Lario S.r.l., Via al Pascolo, 23,842 Bosisio Parini (LC), Italy.

**Table 1** Steps of the thermal stabilization procedure employed to minimize residual substrate stresses on mirrors

1. Thermal aging at 175 °C for 8 h
2. Finish machining
3. Age again at 175 °C for 8 h
4. Perform three thermal cycles from -190 °C to 150 °C, rates not to exceed 1.7 °C/min
5. Repeat three thermal cycles as in Step 4
6. Diamond turning/polishing
7. Repeat three thermal cycles as in Step 4
8. Repeat three thermal cycles as in Step 4 (validation cycle)

expansion in the material. This type of instability cannot be improved by stress release processes.

Finally, there are other sources of instability that are specific to the environmental change path, such as the rate of temperature change, but have been rarely observed in metals, so they have not specifically targeted by the risk mitigation effort.

## 2.2 Thermal stabilization procedure

T651 temper specifications already include a thermal/mechanical hardening and stabilization procedure performed by the aluminum plate supplier, and consisting of a sequence of “solution heat-treating”, “artificially ageing” and “stress relieving by stretching” processes [2].

While this may be sufficient for less demanding applications, use as optical material requires further stress release cycles to minimize the possibility of surface shape variations [9].

Many stress release procedures are available in the literature. Based on a recommendation by the samples manufacturer, we decided to employ as baseline the one proposed by R. G. Ohl et al. from NASA/Goddard Space Flight Center and successfully applied to the *Infrared Multi-Object Spectrograph (IRMOS)* instrument [10].

The main reasons for choosing this procedure are the similarities between the two projects: same substrate material, observation wavelength in the IR and similar operating temperature (80 K).

The procedure, after adaptation according to the availability of cryotesting and manufacturing facilities, was first applied to LTU-1.

The test took place in 2019, and results were satisfactory, leading to a mirror that did not exhibit any change in optical surface shape, within the reproducibility error of the interferometer used, when measured at room temperature before and after the last verification thermal cycle. A detailed discussion and results of this test have been published elsewhere [4].

Based on the results, the procedure was then validated on the three additional 150 mm samples.

The procedure consists of a series of thermal cycles at high temperature followed by a second series of cold/hot thermal cycles (Table 1). Mirror machining and polishing phases are interspersed with the thermal cycles. A final thermal cycle

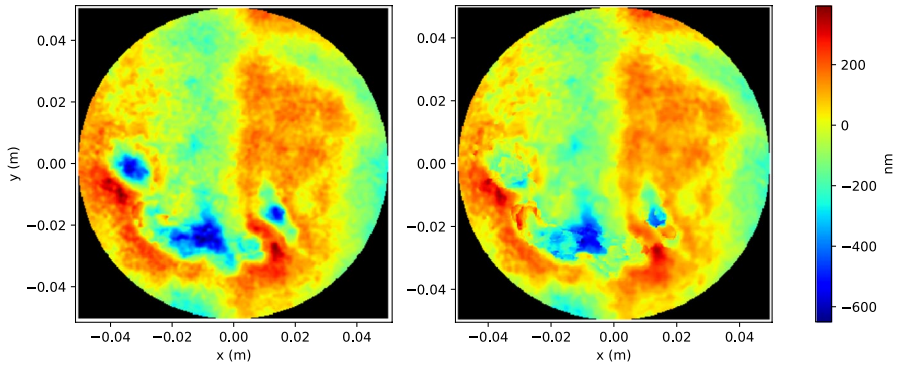


**Fig. 1** Comparison of surface error measurement of the first sample with the Wyko interferometer, before (left) and after (right) the validation thermal cycle

serves as validation step to confirm that the mirror surface reached stability with the required optical shape given by the last polishing phase.

### 2.3 Verification methods

To assess the effectivity of the procedure, the optical surface of the mirrors under test was measured at room temperature before and after each thermal cycle with either a Wyko 8600 Fizeau-type interferometer or a MPR 700 optical profilometer by MediaLario.

If the last thermal cycle of the procedure (validation cycle) had not produce any measurable difference in surface shape, within the reproducibility error of the instrument, the test was deemed as successful.

The comparison of two measurements at room temperature, instead of assessing surface form variation between room and operating temperature, was carried out under the assumption that any release of residual stress would produce a permanent variation in surface shape, and would therefore be detectable also after bringing the sample back at room temperature.

Final qualification of the procedure will then be completed on the prototype of the primary mirror (PTM) with the assessment of the optical surface shape variation between room temperature and operating temperature, validating the assumption stated above.

Surface roughness measurements have been performed with a Taylor Hobson CCI White Light Interferometer (WLI).

### 2.4 Results

The samples underwent the initial hot thermal cycles of the procedure alongside the PTM in a Nabertherm W 2200/A air circulation oven at TAG,<sup>2</sup> and

<sup>2</sup> TAG s.r.l., via Guglielmo Marconi 9, 23,843 – Dolzago (LC) Italy.

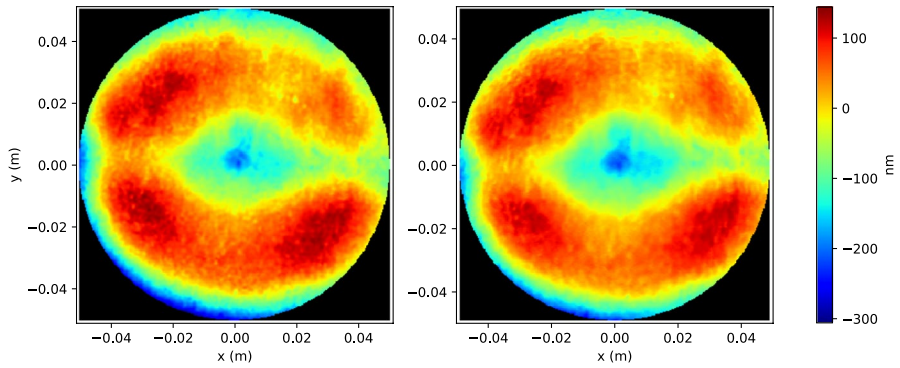


**Fig. 2** Comparison of surface error measurement of the second sample with the Wyko interferometer, before (left) and after (right) the validation thermal cycle

**Fig. 3** Picture of the LamPlan MM8400 flat lapping machine used by MediaLario to test different slurries and pads to set up the polishing procedure

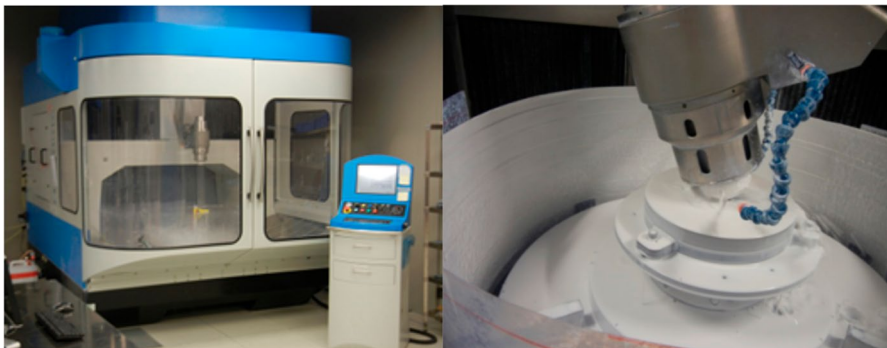
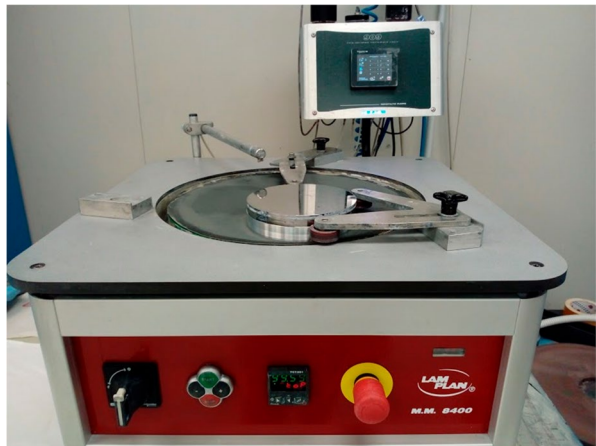


**Fig. 4** Pictures of the Zeeko IRP 1200X robotic polishing machine at MediaLario: ensemble view (left) and close up of the spindle while operating (right)

the cold/hot cycles at INAF-OAS Bologna,<sup>3</sup> at their CryoWaves Lab for the cryogenic part of the cycle and in an Angelantoni CH250 climatic chamber for the hot part of the cycle.

The validation cycle was performed in a thermal vacuum chamber at Criotec Impianti.<sup>4</sup>

In the case of LTU-1, to bring the optical surface to its final shape, an actual fly-cutting process had been applied. For the other three samples, instead, to ease scheduling of the entire validation procedure, figuring was performed through heavy polishing on a LampPlan 8400 polishing machine at MediaLario, and final polishing was performed on a Zeeko IRP 1200 polishing machine, again at MediaLario.

The first measurements of surface error of the samples had been taken before and after the first cold/hot cycle with the MPR 700 optical profilometer (see [15], for a description of the instrument), since the low reflectivity of the unpolished surface was not measurable on the Wyko. Variation in SFE RMS was in the range 0.3–0.9  $\mu\text{m}$ .

The following thermal cycle caused a smaller form variation in the range 0.2–0.6  $\mu\text{m}$ , measured this time with the interferometer.

Final polishing was performed, as anticipated, on the Zeeko IRP1200 using an aggressive procedure in order to bring the form error to specification as much as possible to make form variation assessment more meaningful, while sacrificing surface roughness.

Results were satisfactory on the first two samples, achieving 101 nm RMS and 96 nm RMS of SFE respectively after several polishing runs. For the third sample, polishing had to stop before the required SFE was achieved since by simple visual assessment the optical quality of the surface was degrading so quickly that a serious concern on its interferometric measurability was raised. The sample was then left at 217 nm RMS SFE.

Surface roughness of the three samples, as measured on the Talysurf CCI at 10 $\times$  and 50 $\times$  magnification, was in the range 32–101 nm RMS.

Measurement of the samples using the Wyko interferometer proved anyhow problematic because of surface quality degradation. Eventually, surface shape variation was assessed by comparing a central circular region of 100 mm of diameter, and proved to be within the measurement error for the first two samples: 5 nm RMS and 1 nm RMS respectively, with an error of 10 nm (Figs. 1 and 2). As a comparison, form variation for LTU1, after the last thermal cycle, was  $(6 \pm 10)$  nm.

The third sample showed a larger variation: 26 nm RMS. This result, and the low reflectivity of the sample, prompted further evaluation of the quality of the interferometric measurement. Measurement error on this sample was then assessed to be in the order of 30 nm, higher than the measured difference itself.

A summary of the measurements is presented in Table 2.

<sup>3</sup> INAF-Osservatorio di Astrofisica e Scienza dello spazio di Bologna, Via Piero Gobetti 93/3, 40,129 Bologna, Italy.

<sup>4</sup> Criotec Impianti SpA, Via Francesco Parigi 32/A, 10,034 Chivasso (TO), Italy.

**Table 2** Summary of surface error measurements of the three samples before and after HT5 (validation step of the stress release procedure)

	SFE RMS before validation cycle	FE RMS after validation cycle	Difference
Sample 1	101 nm	96 nm	5 nm
Sample 2	77 nm	76 nm	-1 nm
Sample 3	217 nm	243 nm	26 nm

### 3 Optical surface polishing

Optical surfaces are polished to reduce surface roughness, lowering scattering at the waveband of interest and improving reflectivity. Depending on the process, polishing can also achieve a sufficiently high material removal rate to affect surface shape and mitigate residual surface errors left from the previous machining steps.

Aluminum alloys are notoriously difficult to polish down to less than a few nanometers RMS of surface roughness, and for this reason they are used mostly for IR instruments that have less stringent requirements on surface finish [9]. For this reason, and based on the expertise and manufacturing capabilities of MediaLario, the requirement on surface roughness was set at 10 nm RMS for the qualification phase of the polishing procedure.

Results of directly polishing aluminum alloys are heavily influenced by grain structure and orientation. In particular, polishing of Al6061-T651 in rolled plate form proved particularly difficult because of easy detachment of aggregates of heavy components (such as iron and magnesium) that produce micro-holes and scratches on the surface.

Set up and qualification of a suitable polishing procedure required several iterative steps. For comparison purposes, the tests involved also samples of Al6061-T651 in extruded form, and RSA6061-T6, a rapidly solidified Al alloy from RSP Technology.

The first step was carried out on a flat lapping machine, and consisted in screening existing polishing recipes and setting up a suitable combination of rotating speed, pressure, polishing slurry and pads. Once a promising combination was found, the second step had been transfer of the procedure on the robot polisher. The whole procedure was carried out by MediaLario.

#### 3.1 Optical surface polishing procedure

In order to set up the polishing procedure, several tests were carried out on a LamPlan M8400 flat lapping machine (Fig. 3). The short machine setup time allowed for fast screening of different combinations of pads and slurries to determine the most promising one.

After a good candidate had been identified, the process was transferred to the Zeeko IRP 1200X deterministic polishing machine. The Zeeko consists of a rotating platform on which the piece to polish is secured, and a spindle mounted on a robotic

arm (Fig. 4). The spindle contacts the surface to be polished through an inflatable rubber head covered by a polishing cloth or pad. A lubricating liquid and/or an abrasive slurry are sprayed on the spindle while rotating [17].

The machine operates deterministically, using a surface map of the piece to be polished (usually an interferogram) to determine the optimal polishing path, spindle dwell time on the spots to be polished, rotation speed, angle and inflating pressure.

Small surface form errors can also be corrected in the process, up to a micron on NiP plated mirrors, according to MediaLario experience. Several polishing runs are usually required to achieve the desired shape and surface roughness.

### 3.2 Verification methods

Surface roughness of the polished samples was measured using a Taylor Hobson Talysurf CCI optical profilometer and a Zygo White Light Interferometer (WLI). Measurement spots have been chosen to be representative of the whole surface.

Additional micrographs and SEM–EDX analyses have been performed on the samples during the tests to determine the nature of the imperfections and problematic morphological feature visible on the profilometric images.

In particular, 25 mm diameter samples have been encapsulated in epoxy adhesive and polished in order to perform further metallographic analyses.

Surface form error was measured with a Wyko 8600 Fizeau type interferometer.

### 3.3 Results

#### 3.3.1 Reference results with aggressive polishing process

The first round of tests was performed on the LamPlan MM8400 flat lapping machine (see paragraph 3.1) on a 150 mm sample disk.

Purposes of these initial tests were to perform a baseline characterization of the results obtainable with the aggressive polishing process normally used by MediaLario on aluminum mirrors with an electroless nickel-phosphorous plating, to use as basis for assessing progress, and to study in details any issue than might had appeared.

Results were in fact unsatisfactory: visually, the surface of the sample appeared affected by opacity, and measurements on the Talysurf CCI confirmed the impression, showing that surface roughness was generally higher than the requirement of 10 nm RMS (Fig. 5). In particular, the increased surface roughness seemed to be caused by localized defects, clearly visible at 50× magnification (Fig. 5, center): the areas between defects has instead a roughness below 10 nm RMS (Fig. 5, left).

Appearance of the defects is of holes on a generally even surface, leading to the hypothesis that the aggressive polishing process removed grains of material, probably aggregates of alloy solutes. Additional investigation efforts had then been made to characterize the localized defects, with the aim of guiding the polishing process development effort, using 25 mm aluminum samples.

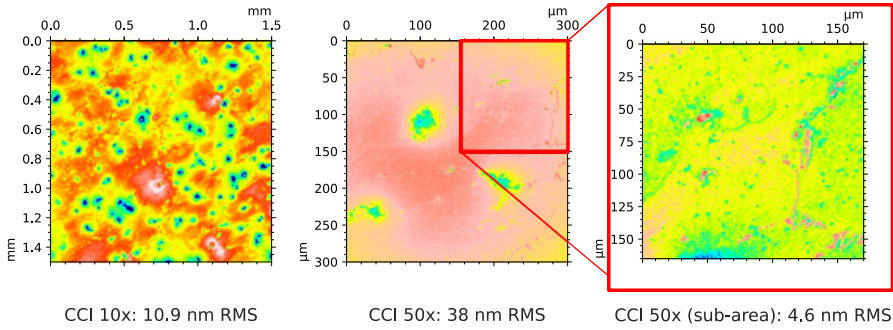


**Fig. 5** Representative roughness measurements of a 6061-T651 rolled plate 150 mm sample, with the aggressive polishing process, taken at different magnifications with the Talysurf CCI optical profilometer. The leftmost picture shows a specific area at 50× magnification with no significant surface defects

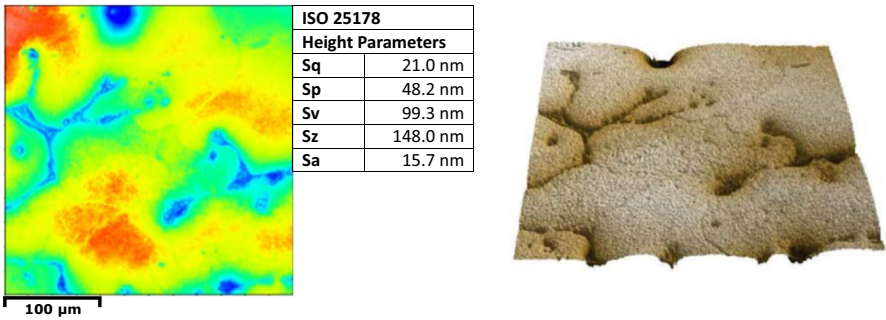


**Fig. 6** 25 mm Al sample after aggressive polishing measured with the Zygo WLI

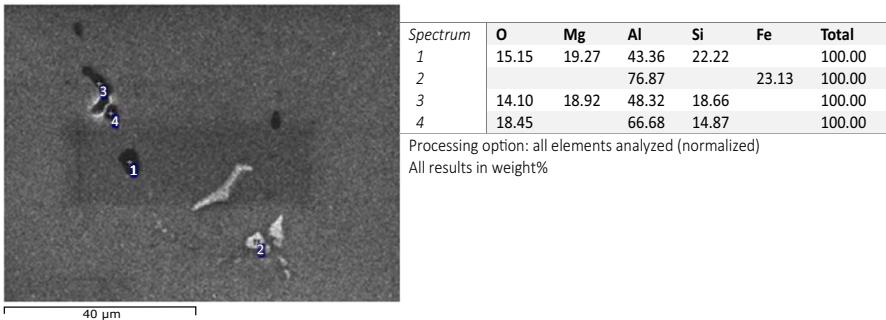


**Fig. 7** SEM–EDX report of the analysis of one of the 25 mm sample in Al 6061-T651

Firstly, the 25 mm samples were measured with a Zygo WLI to confirm that surface morphology after polishing is equivalent to the one obtained on the 150 mm

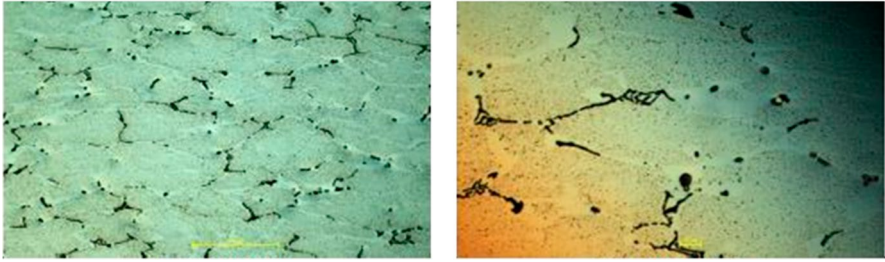


**Fig. 8** Optical micrograph of cross sections of a 25 mm sample subjected to aggressive polishing, at 200X magnification (left) and 500X magnification (right)

samples (Fig. 6). The sample in 6061-T651 rolled plate clearly shows large hollowed structures, also found in the 150 mm samples.

The samples were then analysed with a Scanning Electron Microscope performing Energy-dispersive X-ray spectroscopy (SEM–EDX), as shown in Fig. 7. The analysis identified two kinds of agglomerates: dark areas with generally high concentrations of Mg and Si, and light areas with high concentration of Fe.

Micrographs of the cross-section of the samples (Fig. 8) were also taken, showing that the agglomerate structures are in fact uniformly distributed throughout the material.

### 3.3.2 Final procedure development

The final polishing procedure was developed on the LamPlan, working on 50 mm flat samples of 6061-T651 rolled plate and using a different combination of polishing pad and slurry, and then transferred to the Zeeko IRP1200. The procedure consisted in three polishing phases, with each phase seeing a reduction in removal rate, lowering the pressure of the rotating head and speed at each step.

In the first phase, the 50 mm samples were first lapped to a flatness of approximately 1  $\mu\text{m}$  RMS, while also removing machining marks. The second phase removed the deeper scratches left from the first phase. These two phases used relatively standard tool parameters of rotational speed and pressure applied.

The third phase required more experimentation, as empirical observations highlighted a strong dependence of final roughness on pressure, but eventually results were satisfactory, with roughness in the range of 3–5 nm RMS. A sample measurement of the resulting surface is presented in Fig. 9.

Adapting the identified procedure on the Zeeko required another phase of experimentation with different tool parameters, in particular spindle rotation speed and dwell time, using the same polishing slurry and pad materials identified on the LamPlan.

The final procedure was then tested on the LTU-1 aluminum sample, that had been previously machined flat on a fly-cutting tool. Two polishing runs on the Zeeko were then sufficient to bring the shape error from 220 RMS to 76 nm RMS, within

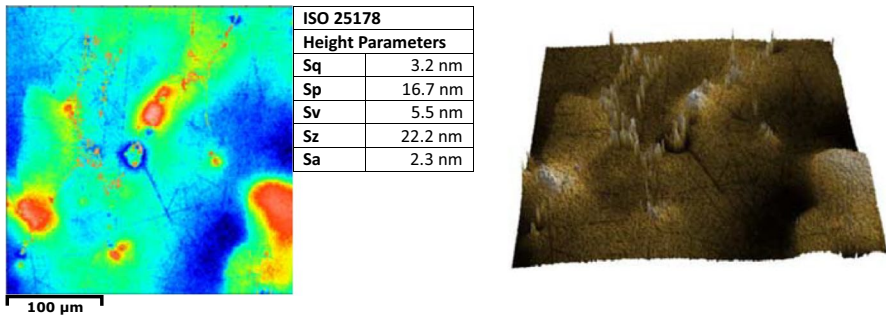


**Fig. 9** Surface roughness measurement on the Zygo WLI of a 50 mm diameter disk of Al6061-T651 rolled plate, polished on the LamPlan using the developed procedure

specifications, and surface roughness to 12 nm RMS, with large areas within the requirement of 10 nm RMS (Fig. 10).

Although the final results on LTU1 were not compliant with the specification of surface roughness, it was decided to proceed anyway with the final test on the PTM itself: the diffuse surface defects identified on the samples polished with the reference procedure were in fact mostly absent with the new process, the removal rate was enough to correct expected shape errors and the polishing runs could be kept within 24 h of duration on the larger PTM surface, allowing reasonable process performance.

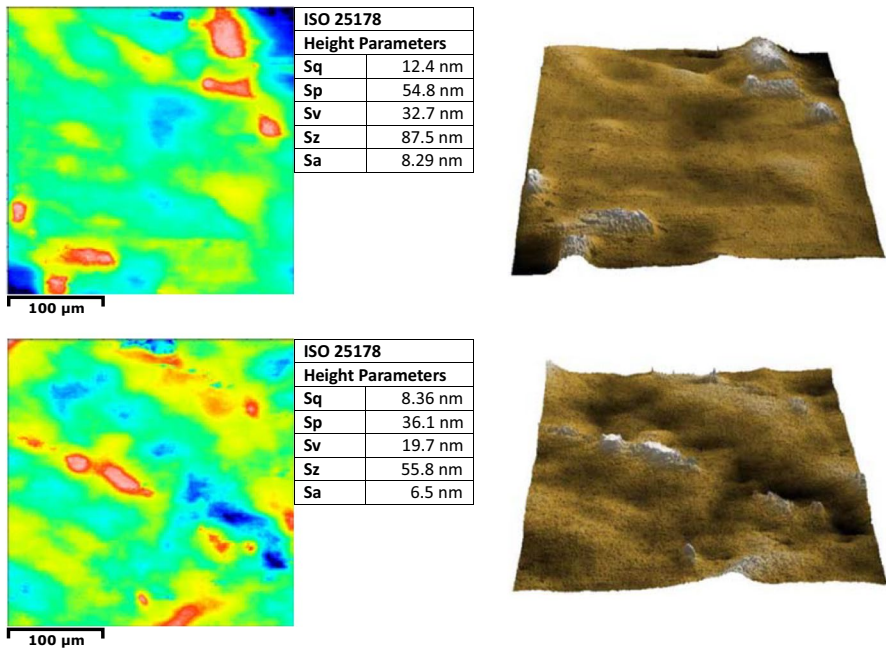


**Fig. 10** Representative surface roughness measurements on the Zygo WLI of the LTU1 Al sample, after applying the final procedure on the Zeeko polishing machine

## 4 Optical surface coating

During Phase A, the ARIEL Consortium decided to apply a protected silver coating to the aluminum mirrors of the telescope to protect them from oxidation and increase reflectivity. The choice of silver, as opposed to gold or aluminum was dictated by the throughput requirement at the operating waveband, with particular regard to the shorter wavelengths.

Protected silver on aluminum substrate has a strong heritage both for ground and space based telescopes, operating also at cryogenic temperatures [3, 13, 14].

A detailed qualification study was nonetheless required because of the large size of ARIEL primary mirror, with particular emphasis on the possible issues caused by process deposition uniformity and CTE mismatch between the specific aluminum alloy used for the mirror substrate and silver.

Another area of concern was the environmental durability of silver, and the effectiveness of the protecting coating layer to avoid exposition and corrosion from common atmospheric pollutants [7, 16].

For the study, a protected silver coating with space heritage from CILAS<sup>5</sup> was selected and tested, mainly based on coating characteristics and capability and availability of the supplier of coating a 1.1 m diameter mirror within the timeframe of the mission.

The study, still ongoing at the time of writing, involves two main activities: a qualification of the coating on aluminum samples, and testing of the coating on the PTM itself. This paper describes the first activity.

### 4.1 Coating process

CILAS coating process is based Physical Vapour Deposition. The coating platform consists in a large magnetron sputtering chamber capable of holding objects up to 2 m by 2 m of footprint, 0.4 m of thickness [8].

The tray holding the samples is able to move back and forth inside the chamber, allowing uniform deposition from the cathodes [12].

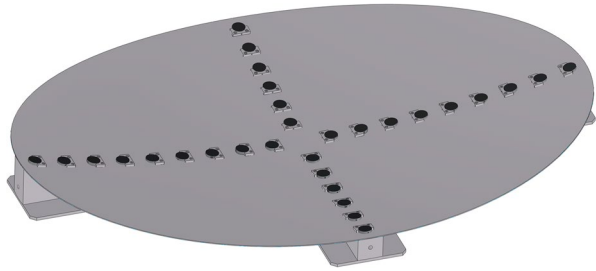
The protected silver coating consists of three layers: an adhesion layer in NiCr, less than 10 nm thick, the silver layer and a dielectric capping and protection layer. The actual coating composition and thickness is a trade secret. The total coating thickness is approximately 350 nm.

### 4.2 Verification methods

A total of 30 samples of 25 mm of diameter were lined up for coating on the major and minor axis of an elliptically shaped sample holder with a curved surface modeled after the optical surface of the PTM (Fig. 11), alternating 11 glass samples and 19 aluminum samples.

<sup>5</sup> CILAS-ArianeGroup, 8 avenue Buffon, CS16319, 45,063 Orleans CEDEX 2, France.

**Fig. 11** Drawing of the samples holder used for the coating deposition, shaped as the PTM optical surface



The 150 mm disks were instead coated lying flat on the coating tray outside of the sample holder. These were used exclusively to test stability of the coating after a series of cryogenic cycles.

Aluminum samples measured surface roughness was generally below 10 nm RMS, with two samples presenting the slightly higher values of 12.1 nm and 11.3 nm RMS. Surface roughness of glass samples had not been measured, but presumed to be less than that of aluminum samples.

After coating, the samples were subjected to a series of environmental (humidity and temperature cycling) and mechanical (adhesion, abrasion) tests to verify stability and performance. Spectral reflectivity, coating thickness and surface roughness have also been measured. A summary of the test specification and equipment used is presented in Table 3.

Visual inspections and relative reflectivity measurements were performed after each test step to identify possible degradation. Reflectivity measurements were limited by instrument availability to a waveband of 0.45–2.5  $\mu\text{m}$  and incidence angles of 8 and 20 degrees, instead of covering the entire ARIEL operating range up to 8  $\mu\text{m}$  and between 3 and 21 degrees AOI. Performance beyond 2.5  $\mu\text{m}$  was positively assessed on a previous coating run, and repeating the measurement was not considered essential, as degradation is most likely to affect reflectivity at lower wavelengths; as for the AOI, results from reflectivity simulations indicated that the available setup would be sufficiently representative of the entire range.

Coating uniformity has also been assessed, both in terms of coating thickness and reflectivity at the lower end of the waveband of interest (500 nm). Glass samples were used for this measurement.

Further ageing tests have been planned to verify stability of the coating and effectiveness of the protection layer in normal storage conditions. These tests are however still ongoing and are not presented here.

#### 4.2.1 Test success criteria

Qualification tests were evaluated according to the following success criteria, applied to the aluminum samples only:

**Table 3** Summary of test specifications and equipment used for coating qualification. All tests were performed at CILAS, unless otherwise indicated

Test	Specifications	Testing equipment
Relative Reflectivity	Wavelength range: 0.45–2.5 μm, AOI 8° and 20°	Perkin-Elmer Lambda 950, calibrated on results from absolute spectral measurements
Visual Inspection	ISO 10110–7	ISO compliant setup with 50 W halogen lamp
Adhesion	ISO 9211–4, Method 2 Severity 2	ISO compliant cellophane tape
Humidity	ISO 9022–2 Method 12 Severity 06 but with a test duration of 24 h: 90% RH, 24 h, 55 ± 3 °C (no condensation)	WEISS, WKL 64/70 climatic test chamber
Temperature cycling at ambient pressure	ISO 9022–2 T. range: -40 °C / +70 °C T. change rate: 2 °C/min Dwell time: 15 min Number of cycles: 30	WEISS, WKL 64/70 climatic test chamber
Abrasion resistance	ISO 9211–4 Method 01 Severity 01	6 mm thick pad of clean, dry cheesecloth
Cryogenic cycling in vacuum	ECSS-Q-ST-70-04C T. range: 54 K / 293 K T. change rate: 5 °C/min Dwell time: 15 min Vacuum: < 10 <sup>-4</sup> mbar Number of cycles: 10	CryoWaves Lab at INAF-OAS Bologna <sup>a</sup>
Coating thickness uniformity	Profilometry on float samples, coated with a mask to expose a ridge between coated surface and substrate	Alpha-Step® D-300 Stylus Profiler KLA Tencor

<sup>a</sup>INAF-Osservatorio di Astrofisica e Scienza dello spazio di Bologna, Via Piero Gobetti 93/3, 40,129 Bologna, Italy

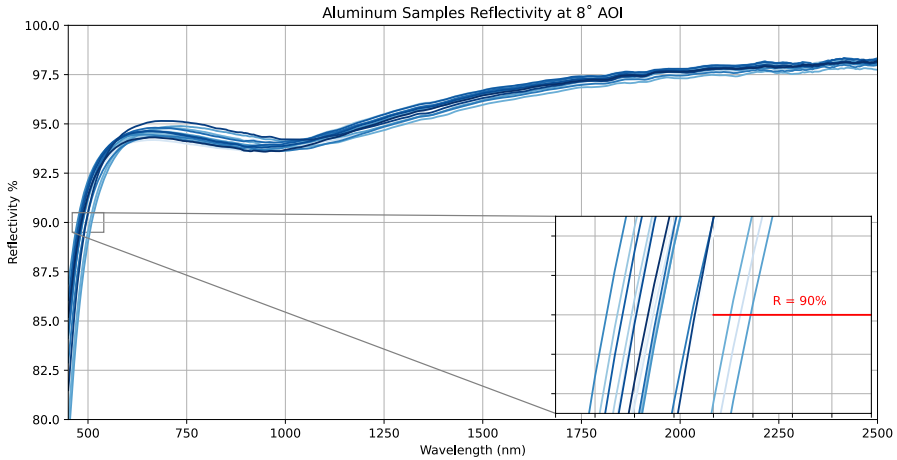


**Fig. 12** Reflectivity of all coated aluminum samples at 8 degrees angle of incidence, and comparison with the requirement of  $R > 90\%$  at wavelengths  $> 500$  nm

1. Reflectivity  $> 90\%$  (goal  $> 95\%$ ) in the  $0.5\text{--}2.5$   $\mu\text{m}$  waveband, best effort in the  $0.45\text{--}0.50$   $\mu\text{m}$  waveband, angles of incidence 8 and 20 degrees.
2. No change in reflectivity, within the measurement reproducibility error, after the tests.
3. No visually detectable signs of degradation or delamination.

The specification on reflectivity is the result of a compromise between mission requirements and the expected performance of the coating, and is applicable to this phase of the qualification campaign only.

Uniformity of coating thickness and uniformity of reflectivity had not been included among the success criteria, but as further means to investigate possible failure, and to provide a baseline characterization of the coating.

### 4.3 Results

Spectral reflectivity was measured at 8 and 20 degrees of angle of incidence, for each sample, at wavelengths up to 2500 nm. The two measurements are identical within the instrument repeatability error, so the following considerations are valid regardless of the angle of incidence of the measurements.

Spectral reflectivity of the aluminum samples was generally above the requirement of 90% for wavelengths greater than 500 nm, as illustrated in Fig. 12, except for three of the outermost samples, positioned at the edge of

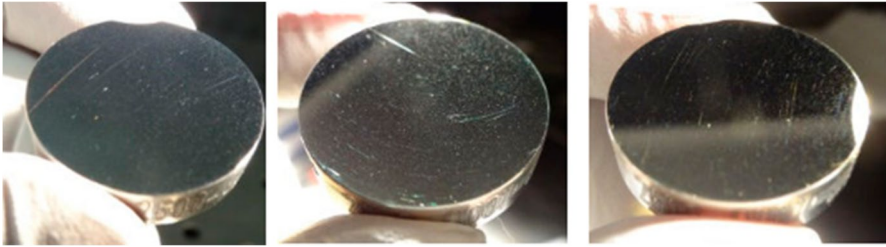


**Fig. 13** Representative pictures of one of the aluminum samples before coating (left), immediately after the coating (middle) and after the tests (right)

three of the four “arms” of the sample holder of Fig. 11. Variation in reflectivity at 500 nm is in the range 89.1%–92.1%.

Glass samples reflectivity is on average higher than aluminum samples by less than 1%, probably due to better surface roughness. Reflectivity uniformity on the glass samples also follows the same trend of the aluminum samples, showing a variation in the range 88.6%–93.6% at 500 nm. The wider range may be explainable by the fact that three of the outermost positions in the holder are occupied by glass samples.

Coating thickness was determined on the glass samples by applying a mask during coating, and measuring the height of the ridge with a profilometer. Samples further away from the center of the holder showed up to 10% higher thickness than the central ones, however no physical relation to reflectivity could be established, and the measurement will only be used for reference with further coating runs.

All mechanical and environmental tests were performed successfully, with no visible sign of delamination or degradation, nor impact on measured spectral reflectivity. A series of representative pictures of the visual appearance of the samples before and after coating and tests can be seen in Fig. 13.

Results of the cryogenic cycles, especially on the larger 150 mm samples, are considered particularly important, since the specific combination of substrate and coating has not been tested at ARIEL operating temperature of 50 K. The coating did not present any visible change in morphology nor changed its spectral reflectivity, leading to conclude that the exposure to high and cryogenic temperatures did no produce any short term degradation. Tape stripping tests were also repeated after the temperature cycles, showing that coating adhesion was not affected.

Finally, reflectivity measurements after the tests showed no variation within instrument accuracy wrt. the measurements taken before the tests.

## 5 Conclusions

The three core processes required to build ARIEL telescope primary mirror, namely substrate thermal stabilization, optical surface polishing and coating were tested on samples of the same aluminum alloy foreseen for the mirror, with the purpose of assessing and improving the level of technological readiness.

Substrate thermal stabilization was successfully verified on two samples. A third sample was found not to be representative due to lower reflectivity affecting the measurement accuracy.

Polishing proved to be particularly difficult, requiring a very delicate and careful process, leading to longer execution times than expected, but eventually the procedure proved to be able to produce the desired results.

Finally, coating reflectivity, although at short wavelengths was slightly lower for the samples at the outer edges of the holder, was on average above specification and therefore compliant with the requirements.

In view of the successful results, the team decided to proceed with the application of the coating to the full size demonstrator of the primary mirror (PTM).

**Funding** Open access funding provided by Istituto Nazionale di Astrofisica within the CRUI-CARE Agreement. This activity has been realized under the Italian Space Agency (ASI) contract with the National Institute for Astrophysics (INAF) n. 2018–22-HH.0, and is partly funded under the ESA contract with Centre Spatial de Liège, Belgium (CSL) and INAF n. 4000126124/18/NL/BW.

**Data availability** The data that support the findings of this study are available from the corresponding author, but restrictions apply to the availability of these data, which were used under license for the current study, and so are not publicly available. Data are however available from the authors upon reasonable request and with permission of the companies and institutions involved in the study.

## Declarations

**Conflicts of interest/Competing interests** The authors declare no conflict of interest.

**Open Access** This article is licensed under a Creative Commons Attribution 4.0 International License, which permits use, sharing, adaptation, distribution and reproduction in any medium or format, as long as you give appropriate credit to the original author(s) and the source, provide a link to the Creative Commons licence, and indicate if changes were made. The images or other third party material in this article are included in the article's Creative Commons licence, unless indicated otherwise in a credit line to the material. If material is not included in the article's Creative Commons licence and your intended use is not permitted by statutory regulation or exceeds the permitted use, you will need to obtain permission directly from the copyright holder. To view a copy of this licence, visit <http://creativecommons.org/licenses/by/4.0/>.


## References

1. Ahmad, A. (ed.): Handbook of optomechanical engineering. CRC Press, Boca Raton (1997)
2. ASM International, Davis, J.R., ASM International eds: Properties and selection: nonferrous alloys and special-purpose materials. ASM International, Materials Park, Ohio (2000)

3. Boccas, M., Vucina, T., Araya, C., Vera, E., Ahhee, C.: Coating the 8-m Gemini telescopes with protected silver. Presented at the SPIE Astronomical Telescopes + Instrumentation, USA (2004)
4. Chioetto, P., Da Deppo, V., Zuppella, P., Pace, E., Morgante, G., Terenzi, L., Brienza, D., Diolaiti, E., Lombini, M., Cortecchia, F., Missaglia, N., Bianucci, G., Spinelli, S., Malaguti, G., Micela, G.: The primary mirror of the ARIEL mission: study of thermal, figuring, and finishing treatments and optical characterization of Al 6061 samples mirrors. In: Hallibert, P., Hull, T.B., and Kim, D.W. (eds.) *Astronomical Optics: Design, Manufacture, and Test of Space and Ground Systems II*. p. 46. SPIE, San Diego, CA, United States (2019)
5. Da Deppo, V., Focardi, M., Middleton, K., Morgante, G., Pascale, E., Grella, S., Pace, E., Claudi, R., Amiaux, J., Colomé Ferrer, J., Hunt, T., Rataj, M., Sierra-Roig, C., FicaïVeltroni, I., Eccleston, P., Micela, G., Tinetti, G.: An afocal telescope configuration for the ESA ARIEL mission. *CEAS Space J.* **9**, 379–398 (2017a). <https://doi.org/10.1007/s12567-017-0175-3>
6. V. Da Deppo et al. “ARIEL telescope material trade-off”, ARIEL-INAF-PL-TN-004, issue 2, (2017b). [https://ARIELspacemission.files.wordpress.com/2017b/05/ARIEL-inaf-pl-tn-004\\_telescope\\_material\\_selection\\_iss-21.pdf](https://ARIELspacemission.files.wordpress.com/2017b/05/ARIEL-inaf-pl-tn-004_telescope_material_selection_iss-21.pdf). Accessed 25 Sept 2020
7. Folgner, K.A., Chu, C.-T., Lingley, Z.R., Kim, H.I., Yang, J.-M., Barrie, J.D.: Environmental durability of protected silver mirrors prepared by plasma beam sputtering. *Appl. Opt.* **56**, C75 (2017). <https://doi.org/10.1364/AO.56.000C75>
8. Grèzes-Besset, C., Valette, N., Chauveau, G., Castelnaud, M., Mathieu, K., Tatat, M., Lemarquis, F.: High performance silver coating with PACA2M magnetron sputtering. In: Karafolas, N., Sodnik, Z., and Cugny, B. (eds.) *International Conference on Space Optics — ICSO 2018*. p. 290. SPIE, Chania, Greece (2019)
9. Newswander, T., Crowther, B., Gubbels, G., Senden, R.: Aluminum alloy AA-6061 and RSA-6061 heat treatment for large mirror applications. In: Robichaud, J.L., Krödel, M., and Goodman, W.A. (eds.) *Proc. SPIE 8837, Material Technologies and Applications to Optics, Structures, Components, and Sub-Systems*, 883704. p. 883704., San Diego, California, United States (2013)
10. Ohl IV, R.G., Barthelmy, M.P., Zewari, S.W., Toland, R.W., McMann, J.C., Puckett, D.F., Hagoopian, J.G., Hylan, J.E., Mentzell, J.E., Mink, R.G., Sparr, L.M., Greenhouse, M.A., MacKenty, J.W.: Comparison of stress relief procedures for cryogenic aluminum mirrors. Presented at the International Symposium on Optical Science and Technology, Seattle, WA November 1 (2002)
11. Puig, L., Pilbratt, G., Heske, A., Escudero, I., Crouzet, P.-E., de Vogeleer, B., Symonds, K., Kohley, R., Drossart, P., Eccleston, P., Hartogh, P., Leconte, J., Micela, G., Ollivier, M., Tinetti, G., Turini, D., Vandenbussche, B., Wolkenberg, P.: The Phase A study of the ESA M4 mission candidate ARIEL. *Exp Astron.* **46**, 211–239 (2018). <https://doi.org/10.1007/s10686-018-9604-3>
12. Savin de Larclause, I., Valette, N., Chauveau, G., Grèzes-Besset, C., Costes, V., Gasc, K., Lemarquis, F.: PACA2m magnetron sputtering silver coating: a solution for very big mirror dimensions. In: Cugny, B., Sodnik, Z., and Karafolas, N. (eds.) *International Conference on Space Optics — ICSO 2014*. p. 177. SPIE, Tenerife, Canary Islands, Spain (2018)
13. Schürmann, M., Gäbler, D., Schlegel, R., Schwinde, S., Peschel, T., Damm, C., Jende, R., Kinast, J., Müller, S., Beier, M., Risse, S., Sang, B., Glier, M., Bittner, H., Erhard, M.: Manufacturing and coating of optical components for the EnMAP hyperspectral imager. Presented at the SPIE Astronomical Telescopes + Instrumentation, Edinburgh, United Kingdom July 22 (2016)
14. Sheikh, D.A.: Improved silver mirror coating for ground and space-based astronomy. Presented at the SPIE Astronomical Telescopes + Instrumentation, Edinburgh, United Kingdom July 22 (2016)
15. Sironi, G., Citterio, O., Pareschi, G., Negri, B., Ritucci, A., Subranni, R., Orlandi, A., Borghi, G., Stroebel, M., Arnold, J., Widemann, R.: MPR: innovative 3D free-form optics profilometer. Presented at the SPIE Optical Engineering + Applications, San Diego, California, USA September 8 (2011)
16. Sytchkova, A., Schwinde, S., Protopapa, M.L., Palmisano, M., Piegari, A., Schürmann, M., Kaiser, N.: Optical characterisation of silver mirrors protected with transparent overcoats. In: Lequime, M., Macleod, H.A., and Ristau, D. (eds.) *Advances in Optical Thin Films VI*. p. 22. SPIE, Frankfurt, Germany (2018)
17. Walker, D.D., Beaucamp, A.T.H., Brooks, D., Doubrovski, V., Cassie, M.D., Dunn, C., Freeman, R.R., King, A., Libert, M., McCavana, G., Morton, R., Riley, D., Simms, J.: New results from the Precessions polishing process scaled to larger sizes. Presented at the SPIE Astronomical Telescopes + Instrumentation, USA September 24 (2004)
18. Kroes, G., Oudenhuisen, A., Meijers, M. & Pel, J.W. MIRI-JWST spectrometer main optics optomechanical design and prototyping. In *Proc. SPIE 5877, Optomechanics 2005* (ed. Hatheway, A. E.) 58770P (2005). <https://doi.org/10.1117/12.614784>

**Publisher's note** Springer Nature remains neutral with regard to jurisdictional claims in published maps and institutional affiliations.

## Authors and Affiliations

**Paolo Chioetto**<sup>1,2,3</sup>  · **Paola Zuppella**<sup>1,3</sup> · **Vania Da Deppo**<sup>1,3</sup> · **Emanuele Pace**<sup>4</sup> · **Gianluca Morgante**<sup>5</sup> · **Luca Terenzi**<sup>5</sup> · **Daniele Brienza**<sup>6</sup> · **Nadia Missaglia**<sup>7</sup> · **Giovanni Bianucci**<sup>7</sup> · **Sebastiano Spinelli**<sup>7</sup> · **Elisa Guerriero**<sup>7,8,9</sup> · **Massimiliano Rossi**<sup>7</sup> · **Catherine Grèzes-Besset**<sup>10</sup> · **Colin Bondet**<sup>10</sup> · **Grégory Chauveau**<sup>10</sup> · **Caroline Porta**<sup>10</sup> · **Giuseppe Malaguti**<sup>5</sup> · **Giuseppina Micela**<sup>9</sup> · **the ARIEL Team**

✉ Paolo Chioetto  
paolo.chioetto@pd.ifi.cnr.it

- <sup>1</sup> CNR-Istituto Di Fotonica E Nanotecnologie Di Padova, Via Trasea 7, 35131 Padova, Italy
- <sup>2</sup> Centro Di Ateneo Di Studi e Attività Spaziali “Giuseppe Colombo”- CISAS, Via Venezia 15, 35131 Padova, Italy
- <sup>3</sup> INAF-Osservatorio Astronomico Di Padova, Vicolo dell’Osservatorio 5, 35122 Padova, Italy
- <sup>4</sup> Dipartimento Di Fisica Ed Astronomia-Università Degli Studi Di Firenze, Largo E. Fermi 2, 50125 Firenze, Italy
- <sup>5</sup> INAF-Osservatorio Di Astrofisica E Scienza Dello Spazio Di Bologna, Via Piero Gobetti 93/3, 40129 Bologna, Italy
- <sup>6</sup> INAF-Istituto Di Astrofisica E Planetologia Spaziali, Via Fosso del Cavaliere 100, 00133 Roma, Italy
- <sup>7</sup> Media Lario S.R.L., Località Pascolo, 23842 Bosisio Parini (Lecco), Italy
- <sup>8</sup> Dipartimento Di Fisica E Chimica-Università Degli Studi Di Palermo, Via Archirafi 36, 90128 Palermo, Italy
- <sup>9</sup> INAF-Osservatorio Astronomico Di Palermo, Piazza del Parlamento 1, 90134 Palermo, Italy
- <sup>10</sup> CILAS-ArianeGroup, Etablissement de Marseille, 600 avenue de la Roche FourcadePôle ALPHA Sud - Z.I. Saint Mitre, 13400 Aubagne, France